Magnetic SPION Retention in Asymmetric Vascular Bifurcation Models

Daniel Fleischhauer
Institute of Polymer Technology
Friedrich-Alexander-Universität Erlangen-Nürnberg
Erlangen, Germany
daniel.fleischhauer@fau.de

Samuel Schlicht
Institute of Polymer Technology
Friedrich-Alexander-Universität Erlangen-Nürnberg
Erlangen, Germany
samuel.schlicht@fau.de

Dietmar Drummer
Institute of Polymer Technology
Friedrich-Alexander-Universität Erlangen-Nürnberg
Erlangen, Germany
dietmar.drummer@fau.de

***Abstract*— Superparamagnetic iron oxide nanoparticles (SPIONs) represent an emerging platform in various fields of nanomedicine. In particular, nanoparticle-based drug delivery techniques that exploit the magnetic properties of SPIONs for targeted transport and accumulation in tumor tissue show considerable promise for cancer therapy. The development of such approaches requires a detailed understanding of how hydrodynamic particle transport, magnetically induced forces, and vascular geometry interact. In this work, we investigate the transient, geometry-induced distribution of SPIONs in generalized vascular structures under magnetic field application. Using statistical scaling laws and empirical data, asymmetric vascular geometries were derived, exhibiting characteristic asymmetry-related vessel diameters. These generalized vascular structures were fabricated via digital light processing (DLP) additive manufacturing and were subsequently tested under magnetic field on and magnetic field off conditions. Optical *in situ* measurements based on the extinction of transmitted light demonstrated a significant influence of geometry and daughter-vessel diameter on transient particle distribution. Since magnetic forces depend on both the underlying flow field and local SPION concentration, these findings suggest an artery-size-dependent boundary for effective magnetic retention under low wash-out conditions.**

Keywords—magnetic drug targeting, test bench, particle propagation, nanoparticles

I. Introduction

Conventional chemotherapy is often limited by systemic toxicity and insufficient drug accumulation at tumor sites. Magnetic drug targeting offers a promising alternative by enabling localized drug accumulation while reducing systemic side effects. Superparamagnetic iron oxide nanoparticles (SPIONs) are particularly suitable carriers due to their surface functionalizability and non-invasive manipulation via external magnetic fields [1]. However, efficient magnetic field dependent SPION retention within the vasculature remains challenging. Nanoparticle transport is governed by competing hydrodynamic, gravitational, and magnetic forces, whose interaction strongly depends on vascular geometry [2,3]. At bifurcations, local flow velocities and shear forces determine particle distribution and emerging flow regimes. While these effects have been studied theoretically and computationally, experimental validation under controlled, physiologically relevant conditions is still limited [4]. To address this gap, we present a generalized, geometrically biosimilar test environment that enables systematic investigation of SPION transport in asymmetric vascular structures. Using optically accessible models fabricated by additive manufacturing, we analyze the transient branch-wise distribution of SPIONs under varying magnetic field conditions.

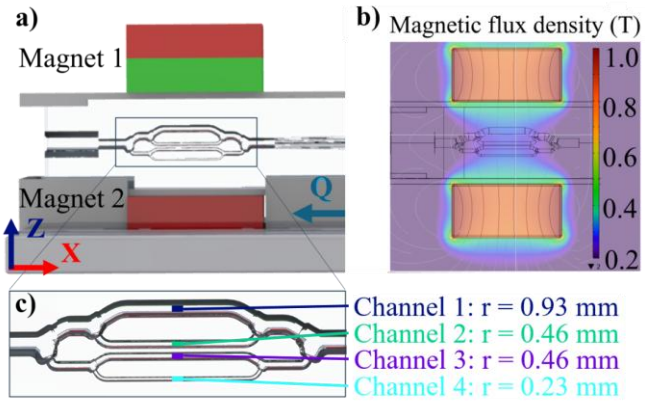

Fig 1: a) Representation of the specimen and magnetic setup according to case 1 as viewed by the camera. b) Representation of the applied magnetic field. c) Illustration of the evaluation positions within the channels and respective channel radii.

II. Methods

A. Specimen Design and Manufacturing

Generalized asymmetric branching structures were derived based on self-similar scaling laws of vascular structures described in the literature. This enables a cross-scale description of the model geometry based on the initial conditions of a few key geometric parameters. According to Murray's law, the relationship between parent- (r_0) and daughter vessel (r_1, r_2) radii is described as follows [5]:

$$r_0^{\alpha} = r_1^{\alpha} + r_2^{\alpha} \tag{1}$$

Depending on tissue type, exponent values between 2 and 3 have been found, with 2.7 ($\approx$ e) reported as optimal for elastic-muscular arteries [6]. The vessel segment radius is linked to the segment length l by a similar proportionality law corresponding to physiological geometries [7]. For asymmetric branching, branching angles change according to daughter vessel size ratios, with angles dependent on parent and daughter vessel radii according to [8]. Branching angles were calculated based on an asymmetry ratio of 0.5 between daughter vessels. Boundary conditions were chosen based on imaging data for breast tumor vascular feeding systems: an entering diameter of 2.5 mm and initial segment length of 12.5 mm. Using these values and relationships, branching models were calculated accordingly.

Such vascular models were manufactured on a digital light processing 3D printer using a transparent standard resin according to the protocol described in [9].

B. Testbench Setup

Experiments were done in an optically accessible flow setup with upstream peristaltic pumping and imaging-based extinction analysis reported in [9]. Blood flow was simulated by distilled water at a flow rate of 5 mL min^{-1}. Before the sample, 0.1 mL of colloidal suspension (10 mg mL^{-1}) was injected. Specimens were positioned with the branching plane aligned to the x-z-plane (Fig. 1). The two NdFeB magnets positioned above and below the specimen at 25 mm distance, yielded a flux density of 350 mT at the geometric center of the specimens. Camera recordings were evaluated for particle propagation by analyzing the transient pixel extinction at defined points in the second-order branches. Relative extinction was calculated with respect to the pre-injection baseline intensity of the water-filled channel at the same ROI. Peak extinction denotes the local maximum of the transient relative extinction signal. Two configurations were tested, which included specimens with the higher-diameter branch positioned uppermost (case 1) as well as positioned with the lower-diameter branch uppermost (case 2), both with and without magnetic field application.

III. Results and Discussion

A. Particle propagation

After injection, particles sediment rapidly to the channel bottom until reaching the first bifurcation. In case 1, despite bottom accumulation, strong extinction signals occur in the upper channels, indicating that higher flow and lower resistance in the upper branch favors particle transport and offsets sedimentation. Upper branches show slightly faster onset compared to channel 3, which exhibits a broader peak due to slower flow velocities. Channel 4 shows significantly delayed, slow onset with a broad peak, indicating slow flow, high resistance, and preference for channel 3 in the lower branch, highlighting the influence of flow distribution and local flow velocites on the particle distribution and signal duration. For Case 2 one pronounced peak occurs in the lowest channel while channel 3 shows only a delayed, weak signal, indicating stratified particles take the high-flow branch. Few particles entering channel 3 suggest disturbances at the branching without significantly offsetting sedimentation.

B. Magnetic field influence

Differences between both cases also show with magnetic field application. Case 2 shows no differences in particle distribution; the large lower channel remains preferred and no particle trapping occurs as extinction decays to initial levels. For case 1, channel 1 exhibits a pronounced particle signal with slower decay compared to the magnet-free condition. Channels 3 and 4 show pronounced signals with faster onset in channel 4 relative to the situation without magnet. While channel 1 flushes out over time, signals in channels 3 and 4 reach a plateau. This persistent deviation from the pre-injection level indicates a macroscopically represented degree of magnetic retention. Particle retention in weak magnetic fields suggests magnetic volume effects exploitable in low-flow vessels. These results indicate a relationship between geometry-induced flow distribution, resulting flow velocities, and magnetic retention capabilities. In particular magnetic

Funded by Deutsche Forschungsgemeinschaft (German Research Foundation) under the grant number 509922606 - GRK 2950: Synthetic Molecular Communication Across Different Scales: From Theory to Experiments, sub-project P06.

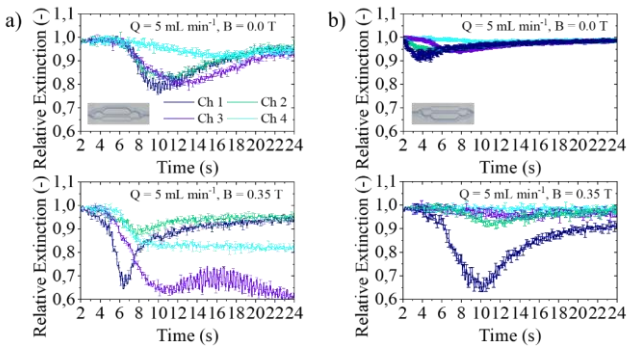

Fig 2: a) Representation of the extinction curves of case 1 without (top) and with (bottom) magnetic setup. b) Representation of the extinction curves of case 2 without (top) and with (bottom) magnetic setup.

retention becomes observable only when local washout is sufficiently weak and residence times are long enough for magnetic forces to act over a relevant duration.

IV. Conclusion and Outlook

The present work shows the influence of locally varying, geometry-induced flow conditions on the duration and shape of the particle signal. Based on the mathematical description of the channel geometry, coupling with simulative data on the flow distribution within the sample will allow for the prediction of signal shape and duration and comparison with the experimental data. Thus allowing for the calculation of a fitting function to correlate the signal shape and magnetic field influence to applied geometric parameters.

Acknowledgment

We thank Prof. Stefan Lyer, University Hospital Erlangen, for providing SPIONs and for fruitful discussions.

References

[1] S. Lyer, R. Singh, R. Tietze, and C. Alexiou, "Magnetic Nanoparticles for Magnetic Drug Targeting," *Biomedical Engineering/ Biomedizinische Technik*, vol. 60, no. 5, pp. 465-475, 2015.

[2] M. Krüger and S. Kopp, "Tumor Models and Drug Targeting In Vitro-Where Are We Today? Where Do We Go from Here?," *Cancers*, vol. 15, no. 6, 2023, doi: 10.3390/cancers15061768

[3] X. Hu, Z. Yang, and Y.-F. Chen, "Fluid-driven particle transport patterns in a confined geometry: Effect of flow velocity and particle concentration," *Journal of Natural Gas Science and Engineering*, vol. 92, p. 103998, 2021, doi: 10.1016/j.jngse.2021.103998.

[4] Sharma, S., Katyar, V.K., and Singh, U. "Mathematical modelling for trajectories of magnetic nanoparticles in a blood vessel under magnetic field." Journal of Magnetism and Magnetic Materials, vol. 379, pp. 102-107, 2015.

[5] C. D. Murray, "The Physiological Principle of Minimum Work: I. The Vascular System and the Cost of Blood Volume," vol. 12, pp. 207-214, 1926.

[6] R. Gödde and H. Kurz, "Structural and biophysical simulation of angiogenesis and vascular remodeling," *Developmental dynamics : an official publication of the American Association of Anatomists*, vol. 220, no. 4, pp. 387-401, 2001, doi: 10.1002/dvdy.1118.

[7] Y. Nakamura and S. Awa, "Radius exponent in elastic and rigid arterial models optimized by the least energy principle," Physiological reports, vol. 2, no. 2, e00236, 2014, doi: 10.1002/phy2.236.

[8] E. Tekin, D. Hunt, M.G. Newberry and V.M. Savage, "Do Vascular Networks Branch Optimally or Randomly across Spatial Scales?," PLoS Comput Biol vol. 12, no.11, e1005223, 2016.

[9] D. Fleischhauer, S. Schlicht and D. Drummer, „Generalized blood vessel models for magnetic nanoparticle-based oncology: geometric and microfluidic properties," Scientific Reports vol. 16, no. 3701, 2026, doi: 10.1038/s41598-026-37348-7.